Safe CO2 threshold limits for indoor long-range airborne transmission control of COVID-19

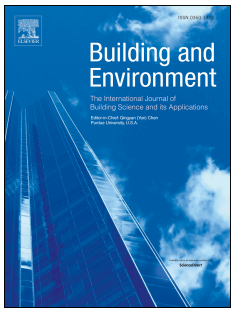

Safe CO_2 threshold limits for indoor long-range airborne transmission control of COVID-19

Xiaowei Lyu, Zhiwen Luo, Li Shao, Hazim Awbi, Samuele Lo Piano

PII: S0360-1323(22)01197-0

DOI: https://doi.org/10.1016/j.buildenv.2022.109967

Reference: BAE 109967

To appear in: *Building and Environment*

Received Date: 15 October 2022

Revised Date: 16 December 2022

Accepted Date: 29 December 2022

Please cite this article as: Lyu X, Luo Z, Shao L, Awbi H, Lo Piano S, Safe CO_2 threshold limits for indoor long-range airborne transmission control of COVID-19, *Building and Environment* (2023), doi: https://doi.org/10.1016/j.buildenv.2022.109967.

Manuscript revised to Building and Environment, Dec 2022

Safe CO_2 Threshold Limits for Indoor Long-range Airborne Transmission Control of COVID-19

Xiaowei Lyu[1], Zhiwen Luo[2]*, Li Shao[1], Hazim Awbi[1], Samuele Lo Piano[1]

1. School of the Built Environment, University of Reading, UK

2. Welsh School of Architecture, Cardiff University, UK

Correspondence: Prof Zhiwen Luo (LuoZ18@Cardiff.ac.uk)

Abstract: CO_2-based infection risk monitoring is highly recommended under the current COVID-19 pandemic. However, the CO_2 monitoring thresholds proposed in the literature are mainly for spaces with fixed occupants. Determining CO_2 threshold is challenging in spaces with changing occupancy due to the co-existence of quanta and CO_2 remaining from the previous occupants. Here, we propose a new calculation framework to derive safe excess CO_2 thresholds (above outdoor level), C_t, for various spaces with fixed/changing occupancy and analyze the uncertainty entailed. Common indoor spaces were categorized into three scenarios according to their occupancy condition, e.g., fixed or varying infection ratios (infectors/occupants). We proved that rebreathed fraction-based model can be directly applied for C_t derivation in the cases of a fixed infection ratio (Scenario 1 and Scenario 2). In the case of varying infector ratios (Scenario 3), C_t derivation has to follow the general calculation framework due to the existence of initial quanta/excess CO_2. Otherwise, significant bias can be

caused for C_t (e.g., 260 ppm) when infection ratio varies remarkably. C_t significantly varies with specific space factors such as occupant number, activities, and community prevalence, e.g., 7 ppm for gym and 890 ppm for lecture hall, indicating C_t should be determined on a case-by-case basis. An uncertainty of C_t up to 6 orders of magnitude was found for all cases due to uncertainty in emissions of quanta and CO_2, thus emphasizing the role of accurate emissions data in obtaining C_t.

Keywords: infection risk control, CO_2 monitoring, initial quanta, uncertainty analysis

Nomenclature

B	Breathing rate, m^3/h
$C_{CO2,i}$	CO_2 concentration for occupancy stage i, ppm
$C_{\mathrm{Cin,i}}$	Initial CO_2 concentration for occupancy stage i, ppm
$C_{q,i}$	Quanta concentration for occupancy stage i, quanta/m^3
$C_{qin,i}$	Initial quanta concentration for occupancy stage i, quanta/m^3
C_t	Safe excess CO_2 threshold, ppm
C_{t50}	Median safe excess CO_2 threshold, ppm
E_{co2}	CO_2 emission rate, mL/s
E_q	Quanta emission rate, quanta/h
I_i	Infector number for occupancy stage i
N_{ave}	Average occupant number
N_i	Occupant number for occupancy stage i
P_i	Infection risk for occupancy stage i
P_t	Predefined infection risk threshold
P_I	Community prevalence
T_i	Exposure time for occupancy stage i, h
V	Space volume, m^3
λ_i	Air change rate for occupancy stage i, h^{-1}

1. Introduction

COVID-19, as a novel coronavirus disease, has caused a worldwide pandemic spreading since the end of 2019 (Chen et al., 2020). Indoor transmission control is the key to prevent the spread of the SARs-CoV-2 virus due to a higher transmission risk indoors than outdoors (Qian et al., 2020). The four main transmission routes in indoor environments are droplet-borne, fomite, short-range airborne, and long-range airborne (Li, 2021; Wei and Li, 2016). Although short-range airborne transmission route was inferred to be the dominant route in close contact (Chen et al., 2020), long-range airborne transmission was revealed to more likely induce outbreaks in poorly ventilated and confined indoor spaces (Peng et al., 2022). Thus, it is of primary importance to monitor and control long-range airborne transmission for indoor environment.

The exhaled infectious aerosols contributing to long-range airborne transmission are difficult to detect, and can travel a long distance in indoor environment. Therefore, a detectable indicator for transmission risk is urgently needed to effectively monitor long-range airborne transmission. CO_2 that can be easily monitored through low-cost sensors (Peng and Jimenez, 2021) has been recommended as risk indicator for long-range airborne transmission because it can both reflect the indoor ventilation condition and the quanta concentration (Persily et al, 2022). Accordingly, safe CO_2 thresholds are defined as the maximum CO_2 concentration level under which the indoor space is at an acceptable infection risk. Such information is useful to guide the design of infection-resilient buildings.

Treating CO_2 as an indicator for indoor ventilation performance, recent studies made use of CO_2 thresholds for risk control based on prevailing ventilation standards with a target of acceptable indoor air quality (IAQ) but not infection risk (CIBSE, 2021; SAGE-EMG, 2021;

REHVA, 2021). ASHRAE does not recommend a specific value of threshold (Persily et al., 2022), although other organizations have suggested specific thresholds of 800 ppm (SAGE-EMG, 2020; CDC, 2021) or 800-1000 ppm (REHVA, 2021) to ensure a safe indoor environment. However, whether a fixed CO_2 threshold could guarantee a low infection risk for all spaces is questionable considering factors such as occupancy level and respiratory activity can all affect the value of it (Peng and Jimenez, 2021).

Moving beyond the assessment of CO_2 as a mere indicator of indoor ventilation condition, CO_2 can also be used to directly reflect quanta concentration as CO_2 and virus-laden aerosols can be co-produced and co-inhaled by human. Therefore, CO_2 thresholds can be calculated backward by pre-defining an acceptable infection risk level (Hou et al., 2021; Peng and Jimenez, 2021). Indoor airborne transmission risk can be maintained under the predefined risk level in as much indoor CO_2 concentration can be maintained below the derived threshold. Occupancy level and respiratory activity for a particular indoor space can all be factored in this backward calculation process (Hou et al., 2021; Peng and Jimenez, 2021; Rudnick and Milton, 2003). In the literature, the derived thresholds were found to be highly sensitive to factors such as activity level and community prevalence, making CO_2 thresholds varying across different indoor spaces (Peng and Jimenez, 2021). For example, the reference excess CO_2 threshold (above outdoor level) for classroom amounts to only about 150 ppm, while this figure is ten-fold for supermarket (Peng and Jimenez, 2021). This indicates that the CO_2 thresholds should be determined case by case, instead of setting a fixed value for all spaces.

In addition, most proposed thresholds are for spaces with fixed occupancy level under the assumption of no initial quanta/excess CO_2 (Hou et al., 2021; Peng and Jimenez, 2021; Rudnick

and Milton, 2003). For spaces with variable occupancy, some of quanta/CO_2 released by the previous group of occupants can remain in the space and become initial quanta/CO_2 when the next group occupies the space, hence increasing the infection risk for the current occupants. The initial quanta is essential for defining CO_2 threshold, but it is difficult to estimate as it requires information of ventilation condition and occupancy profile of previous occupancy stage. Hence, how to account for initial quanta/excess CO_2 in spaces with changing occupancy in infection risk assessment remains an unsolved question (Mittal et al., 2020b; Wei and Li, 2016).

Finally, emissions of quanta and CO_2 are two important parameters in determining the CO_2 threshold, but they have inter-individual variation and can also be affected by factors such as age and gender (Buonanno et al., 2020a; Persily and de Jonge, 2017; Good et al., 2021). For instance, the viral load of super-spreader can be 10 times higher than the mean level of normal infectious subjects (Lelieveld et al., 2020), which may indicate a higher quanta emission (Ke et al., 2021, 2022). Different values of quanta and CO_2 emission were adopted by previous studies for CO_2 threshold derivation, e.g., from 0.37 quanta/h to 100 quanta/h for classrooms (Buonanno et al., 2020a; Bazant et al., 2021; Hou et al., 2021; Peng and Jimenez, 2021). The effect on the uncertainty on the emissions of quanta and CO_2 on defining a CO_2 threshold should be further analyzed. The present study aims to provide a new calculation framework to derive safe excess CO_2 thresholds (C_t) by considering initial quanta/excess CO_2 and changing/fixed occupancy patterns for different indoor spaces, as well as propagating the uncertainty of these input variables.

2. Methodology

98 *2.1 General calculation framework*

99 Our model is based on four assumptions for indoor mass balance equations for CO_2 and
100 quanta (Hou et al., 2021): 1) both CO_2 and quanta are well mixed and evenly distributed in
101 the air; 2) indoor excess CO_2 is released by human exhalation only, with no other indoor
102 sources; 3) CO_2 emission rate and quanta emission rate are both constant (i.e., not time
103 dependent); 4) the loss of quanta is mainly due to ventilation, other elimination mechanisms
104 such as deposition, filtration and inactivation are neglected.

105 In deriving C_t for spaces with changing occupants, we consider a sequence of occupancy
106 stages, $S_i(I_i, N_i, T_i)$. Stage i represents an indoor space (with the volume of V) being occupied
107 by a number of occupants (N_i) with infectors (I_i) for a duration of time (T_i). i =1 represents the
108 start of the occupancy: N_1 occupants (with I_1 infectors) stay in this indoor space for a period of
109 T_1, with no people inside prior to N_1 occupants. The introduction of various occupancy stages
110 aims to consider the virus released and still in the air from previous occupancy stages (the
111 initial quanta). This is fundamentally different from previous studies which only considered
112 one-off occupancy or fixed occupancy throughout the exposure period of interest.

113 The general calculation process of C_t for one occupancy stage of a space is given as follows.

114 Long-range transmission risk for occupancy stage i is modeled through a Wells-Riley model
115 (Riley et al., 1978) amended by Gammitoni and Nucci (1997) to assess infection risk through
116 unsteady-state quanta concentration:

117 $$P_i = 1 - e^{-B\int_0^{T_i} C_{q,i}(t)dt} \quad (1)$$

118 Quanta concentration in Equation (1) is modeled through transient mass balance equation:

119 $$\frac{dC_{q,i}}{dt} = \frac{I_i E_q}{V} - \lambda_i C_{q,i} \quad (2)$$

Equation (2) can be analytically solved as:

$$C_{q,i}(t) = \left(C_{\text{qin,i}} - \frac{I_i E_q}{\lambda_i V}\right) e^{-\lambda_i t} + \frac{I_i E_q}{\lambda_i V} \quad (3)$$

To control transmission risk of stage *i* under an acceptable low level, a risk threshold of P_t needs to be initially determined. Based on P_t, a required ACH (air change rate, λ_i) can be derived by substituting Equation (3) into Equation (1), λ_i should be no less than the derived value to keep transmission risk under P_t.

Indoor excess CO_2 concentration is also dominated by ACH, hence it reflects the ventilation condition of stage *i*.

Indoor excess CO_2 concentration for stage *i* is determined by mass balance equation (4):

$$\frac{dC_{CO2,i}}{dt} = \frac{N_i E_{CO2}}{V} - \lambda_i C_{CO2,i} \quad (4)$$

Equation (4) is solved as:

$$C_{CO2,i}(t) = \left(C_{Cin,i} - \frac{N_i E_{CO2}}{\lambda_i V}\right) e^{-\lambda_i t} + \frac{N_i E_{CO2}}{\lambda_i V} \quad (5)$$

Substituting the required ACH that is backward calculated from transmission risk threshold into Equation (5), the time-averaged indoor excess CO_2 concentration ($C_{CO2,i}$) during T_i is exactly C_t for stage *i* (Hou et al., 2021; Bazant et al., 2021):

$$C_t = \frac{1}{T_i}\int_0^{T_i} C_{CO2,i}(t)dt \quad (6)$$

When indoor excess CO_2 concentration is below the reference threshold C_t, sufficient ventilation can be promised to keep long-range transmission risk for occupancy stage *i* under the risk level of P_t.

Further, for different occupancy stages, C_t can be derived by following the steps mentioned above considering the existence of initial quanta/excess CO_2, see Equation (3) and Equation (5). Starting from occupancy stage 1 without initial quanta/excess CO_2, a required ACH (λ_1)

can be easily obtained following the general calculation process. For occupancy stage 2, the initial quanta and initial excess CO_2 can be estimated based on the ACH derived in occupancy stage 1 (λ_1) under the assumption that excess CO_2 during occupancy stage 1 has been controlled under the reference threshold, C_t for occupancy stage 2 can then be obtained according to the calculation framework. Repeating these steps, i.e. by taking the derived ACH of previous occupancy stage to estimate initial quanta/excess CO_2 for present stage, C_t can be calculated iteratively for all the occupancy stages modeled.

2.1.1 Infection Risk Threshold P_t

The infection risk threshold P_t is of great importance as it dominates the safety levels of the indoor environment. It can be defined in two ways, either by using a constant value for all environment - such as 1%, 0.1% (Dai and Zhao, 2020) or even 0.01% (Peng and Jimenez - 2021) or to determine P_t based on reproductive number (R_A) where R_A is the average number of secondary cases caused by one infector in a given susceptible population in indoor environment. In the latter, the value of P_t is dominated by the number of occupants and can be a large and inconvincible value when occupant number is small (Ma et al., 2018; Furuya et al., 2009). In this study, we use a constant value of P_t = 0.01% as suggested in Peng and Jimenez (2021), which is reasonable for most occupancy stages when the number of occupants is less than 10,000.

2.2 Designed Scenarios

Three scenarios were identified to calculate C_t:

1) Regularly attended space with fixed occupancy level and the same group of people as occupants, so that $N_1=N_2=...$ (e.g., a lecture room used by a certain group of students) (Burridge et al., 2021; Vouriot et al., 2021) ;

2) Non-regularly attended space with constant infection ratio ($I_1/N_1=I_2/N_2=...=I_i/N_i$), different groups of people as occupants, and with high occupancy level (e.g., shopping center, train station);

3) Non-regularly attended space with changing infection ratio ($I_1/N_1\neq I_2/N_2\neq...\neq I_i/N_i$) and low occupancy level (e.g., gym, train coach).

All these scenarios are widely experienced in real-life situations.

2.2.1 Scenario 1: Regularly attended spaces

We determined the number of infectors I_i for Scenario 1 according to both the indoor occupancy level (N_i) and local community prevalence (P_I). The expected I_i is defined as max $\{1, P_IN_i\}$. When with a low indoor occupancy level or a low community prevalence, the value of P_IN_i can be less than 1, under such condition, I_i is assumed to be equal to 1, Otherwise, I_i is assumed to be P_IN_i to reflect the real local infection condition.

Derived from mass balance equations, quanta concentration and excess CO_2 concentration were found to have a constant proportion during all the occupancy stages, only affected by infection ratio and emissions, see Equation (7) (Full derivation details can be found in Supplementary Information). As long as the infection ratio and emissions do not change during the occupancy stages, the proportion remains unchanged as well, hence:

$$\frac{C_{q,1}(t)}{C_{CO2,1}(t)} = \frac{C_{q,2}(t)}{C_{CO2,2}(t)} = \cdots = \frac{I_i}{N_i}\frac{E_q}{E_{CO2}} \quad (7)$$

Under these circumstances, infection risk for stage *i* Eq (1) can be revised as below

$$P_i = 1 - e^{-B\frac{I_i}{N_i}\frac{E_q}{E_{CO2}}\int_0^{T_i} C_{CO2,i}(t)dt} \quad (8)$$

Equation (8) can be treated as the classical rebreathed fraction (RF) -based infection risk model derived by Rudnick and Milton (2003), with $BC_{CO2,i}(t)/E_{CO2}$ representing the rebreathed fraction. This derivation proved that rebreathed fraction (RF) -based model can account for the impact of initial quanta/excess CO_2 in risk assessments for spaces with fixed occupants.

Based on Equation (8), the time averaged value C_t for occupancy stage *i* can then be derived as:

$$C_t = \frac{E_{CO2}N_i}{E_q T_i B I_i} ln\left(\frac{1}{1-P_t}\right) \quad (9)$$

2.2.2 Scenario 2: Non-regularly attended spaces with constant infection ratios

In Scenario 2, we assumed that community prevalence (P_I) can be directly used to represent indoor infection ratio due to the high occupancy level ($I_1/N_1=I_2/N_2=\ldots=P_I$). The proportion between $C_{q,i}$ and excess $C_{CO2,i}$ also become constant due to the constant infection ratio among occupancy stages (Detailed derivation process can be found in Supplementary Information):

$$\frac{C_{q,1}(t)}{C_{CO2,1}(t)} = \frac{C_{q,2}(t)}{C_{CO2,2}(t)} = \cdots = P_I\frac{E_q}{E_{CO2}} \quad (10)$$

Similar as Scenario 1, the infection risk and excess CO_2 threshold can then be derived as:

$$P_i = 1 - e^{-BP_I\frac{E_q}{E_{CO2}}\int_0^{T_i} C_{CO2}(t)dt} \quad (11)$$

$$C_t = \frac{E_{CO2}}{E_q T_i B P_I} ln\left(\frac{1}{1-P_t}\right) \quad (12)$$

Equation (11) can be treated as an extension of the classical RF-based infection risk model. The generality of the original model is extended from scenarios with fixed occupants (scenario

1) to scenarios with varying occupancy levels (scenario 2), with initial quanta/excess CO_2 to be taken into account. It should be noted that T_i in Scenario 2 is usually hard to monitor as the occupancy level keeps changing. An alternative method is to predefine it according to the characteristics of different spaces. For example, T_i could be set as 35 min for check-in hall and 100 min for departure hall according to the average dwelling times measured in an airport (Mihi et al., 2018).

2.2.3 Scenario 3: Non-regularly attended spaces with changing infection ratios

In Scenario 3, indoor infection ratio cannot be represented by P_I due to the relatively low occupancy level. I_i is therefore recommended as the maximum value of {1, N_iP_I} to provide a safe indoor environment (as Scenario 1). In these circumstances, the infection ratio would change among the occupancy stages and quanta concentration, and it would not be represented by excess CO_2 concentration: C_t derivation needs to follow the general calculation process (see Part 2.1).

It should be noted that the general calculation process does not require the field measurement of ACH but relies on a known occupancy profile including the number of occupants and the duration of occupancy for all the occupancy stages. Thus, this method may be more suitable for spaces in Scenario 3 where the occupancy profile of N_i and T_i of each occupancy stage can be monitored simultaneously or obtained before the spaces being occupied such as the rail train or theatre.

2.3 Uncertainty analysis and inputs

Uncertainty analysis was carried out considering E_q and E_{CO2} have interindividual variation

and can vary with gender, age, leading uncertainty to C_t. The probability density functions (PDF) of E_q for three different activities are from recent research of Buonanno et al. (2020a), where they found the quanta emission follows a log10-normal distribution, see Table 1. E_{CO2} was also assumed to be lognormally distributed with a standard deviation equal to 20% of its mean (Molina and Jones, 2021). The mean value for the distribution is calculated as the average value of E_{CO2} of female and male individuals aged 30 to 40 years (the most frequent age cohort) with a specific metabolic equivalent (Persily and de Jonge, 2017). The metabolic equivalent for E_{CO2} is specified by different activity levels, specifically, 1.5 met for sedentary activity, 3 met for light activity, 9 met for heavy activity (Ainsworth et al., 2000). Latin Hypercube sampling (LHS) (Fang et al. 2005) was used to generate a total of 30,000 samples from emissions of quanta and CO_2 due to its advantage in reflecting the true underlying distribution of inputs with a smaller sample size. Monte Carlo simulations (Sobol', 1994) were used to propagate and quantify the uncertainty in predictions.

Table 1. Inputs for Uncertainty Analysis. Distribution mean and standard deviation in brackets

Activity	Quanta emission PDF (quanta/h)	CO_2 emission PDF (mL/s)
Sedentary - breathing	LN10 (-0.429, 0.720)	LN (5.05, 1.01)
Light activity - speaking	LN10 (0.698, 0.720)	LN (10.10, 2.02)
Heavy activity - breathing	LN10 (0.399, 0.720)	LN (34.20, 6.84)

Typical indoor environments were selected for each scenario based on factors such as occupancy level, infection ratio etc. (Tables 2 and 3). Cases in Scenario 1 have a fixed but different number of occupants considering that this is a dominant parameter in deriving C_t in Scenario 1, see Equation (9). It should be noted that the case of lecture hall in Scenario 1 has 3 infectors due to its high occupancy level, whereas other cases have only 1 infector due to the

244 relatively low occupancy level. In Scenario 2 a shopping center was taken as case study with
245 variable levels of community prevalence, which were adopted from three different COVID-19
246 periods in the UK for 2020 (Pouwels et al., 2021) to represent relatively small (0.06%), median
247 (0.4%) and high (1%) community prevalence, among which the highest level of community
248 prevalence was adopted for Scenario 1 and Scenario 3. Two cases with low and changing
249 occupancy levels were selected for Scenario 3 (i.e., train coach and gym room). As regards
250 occupancy stages, only one stage was included for cases in Scenario 1 and Scenario 2 whereas
251 five occupancy stages were included for cases in Scenario 3 to take into account the variability
252 in C_t due to the impact of initial quanta/excess CO_2. Different categories of activities were
253 considered in the cases of the different scenarios. Cases in Scenario 1 are assumed to have
254 "sedentary activity - breathing" typical of people sitting or standing in office or classroom
255 environments. Cases in Scenario 2 are assumed to have "light activity - speaking", considering
256 that people are usually walking in the shopping center and talking to each other. For scenario
257 3, two activities are included to explore the effects of activity level on C_t derivation, specifically,
258 "sedentary activity – breathing" for the train coach and "moderate activity – breathing" for
259 gym. The breathing rates (B) corresponding to different physical activity level is adopted are
260 from previous research (*Adams*, 1993).

261 **Table 2. Inputs of uncertainty analysis for Scenario 1 and Scenario 2.**

Case	Volume (m^3)	Infector number	Occupant number	Exposure time (h)	Community prevalence	Breathing rate (m^3/h)
Scenario 1						
Classroom	231	1	30	1	1%	0.54
Lecture classroom	270	1	65	1	1%	0.54
Lecture hall	540	3	300	1	1%	0.54
Open-plan office	594	1	20	1	1%	0.54
Scenario 2						

Shopping center	2040	-	-	1	0.06%, 0.4%, 1%	1.38

Table 3. Inputs of uncertainty analysis for Scenario 3

Scenario 3	Stage 1	Stage 2	Stage 3	Stage 4	Stage 5
Train coach (300 m^3)					
Infector number	1	1	1	1	1
Occupant number	20	40	80	40	20
Exposure time (h)	1	1	1	1	1
Community prevalence	1%	1%	1%	1%	1%
Breathing rate (m^3/h)	0.54	0.54	0.54	0.54	0.54
Gym (600 m^3)					
Infector number	1	1	1	1	1
Occupant number	5	10	20	10	5
Exposure time (h)	1	1	1	1	1
Community prevalence	1%	1%	1%	1%	1%
Breathing rate (m^3/h)	3.30	3.30	3.30	3.30	3.30

3. Results

3.1 Safety excess CO_2 threshold varies in different scenarios

For Scenario 1, the number of occupants (N_i) is the dominant factor governing C_t that scales with it (see Equation (9)). C_t for cases with different N_i in Scenario 1 (regularly attended spaces) have substantial differences, see Figure 1(a). The highest C_{t50} (the median value of C_t) occurs in lecture hall (890 ppm), followed by lecture classroom (580 ppm), classroom (270 ppm), the lowest one is in office environment (180 ppm), although significant overlaps exist in the output distributions (Figure 1(a)).

For Scenario 2, instead of N_i, C_t is dominated by community prevalence (P_I), as C_t is inversely proportional to P_I (see Equation (12)). Three different values of P_I (i.e., 0.06%. 0.4% and 1%) are adopted to derive C_t and the results are showed in Figure 1(b). The highest C_{t50} of 870 ppm refers to the lowest P_I of 0.06% and the lowest C_{t50} of 50 ppm to the highest P_I of 1%.

For Scenario 3, the changing infection ratios lead to different values of C_t for different

occupancy stages. For train coach, C_{t50} are approx. 180 ppm, 320 ppm, 650 ppm, 410 ppm and 200 ppm corresponding to infection ratios of 1/20, 1/40, 1/80, 1/40 and 1/20 for the five stages in sequence, while they are 7 ppm, 15 ppm, 30 ppm, 15 ppm and 7 ppm for gym environment corresponding to infection ratios of 1/5, 1/10, 1/20, 1/10 and 1/5. The changing infection ratios can lead to different C_t values in different stages mainly because the existence of initial quanta/excess CO_2. For instance, for Stage 2 and Stage 4 of train coach with the same occupant number of 40, C_{t50} should be same if initial quanta/excess CO_2 is not considered, but in fact the difference of C_{t50} between the two occupancy stages reaches approx. 80 ppm due to the impact of initial quanta/excess CO_2.

In addition, the general cases in Scenario 3 also proves that activity level is another major factor which can affect the derived thresholds, see Figure 1(c). C_t for gym with a high activity level is much lower than that for train coach with a sedentary activity level due to relative high activity level in gym environment (hence, high emission rate for quanta). This agrees with previous studies (Chen et al., 2022; Jia et al., 2022) that there should be much higher restriction in spaces with high activities such as gym to control airborne infection risk.

Apart from the substantially different C_t among different cases, large uncertainty of C_t was also found in each case, spanning up to six orders of magnitude on a log scale (see Figure 1). Figure 1 shows that cases with a large median value contain more uncertainty due to a more right-shifted log-scaled distribution of C_t, indicating that C_t can be more affected by the uncertainty of emission settings considered in our study. Considering the large uncertainty of C_t and the non-normal distribution when transformed to a linear scale, the median safe excess CO_2 threshold (C_{t50}) is an appropriate descriptive statistic for excess CO_2 threshold due to its

high probability density (see the violin plot in Figure 1) (Jones et al., 2021).

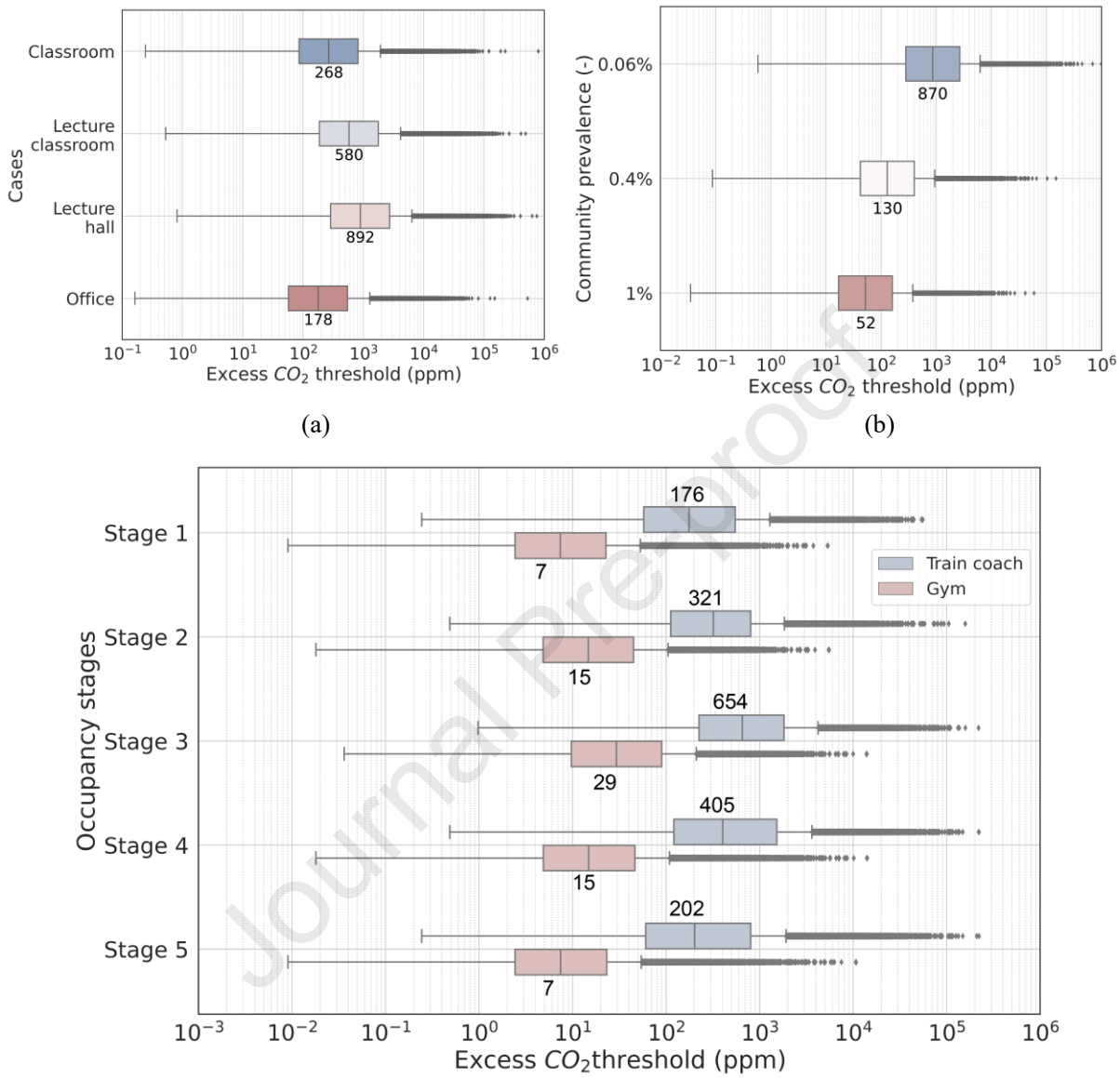

Figure 1. Safe excess CO_2 thresholds for 3 scenarios: (a) Scenario 1(with fixed occupancy); (b) Scenario 2 (with changing occupancy but fixed infection ratios); (c) Scenario 3 (with changing occupancy and non-fixed infection ratios).

3.2 Effect of infection risk threshold (P_t)

As discussed before, the infection risk threshold (P_t) plays a role in deriving C_t. Different P_t

have been adopted in different research in the range of 0.01% to 1% (Buonanno et al., 2020b; Dai and Zhao, 2020; Peng and Jimenez, 2021; Zhang et al., 2021). Here we explore how P_t will affect C_t with results shown in Figure 2. The base case is the classroom in Scenario 1 (see Table 2). C_{t50} is found to be approximately linearly related to P_t with approx. 270 ppm for P_t = 0.01% to 27000 ppm for P_t = 1%, which reveals the high sensitivity of C_{t50} to P_t.

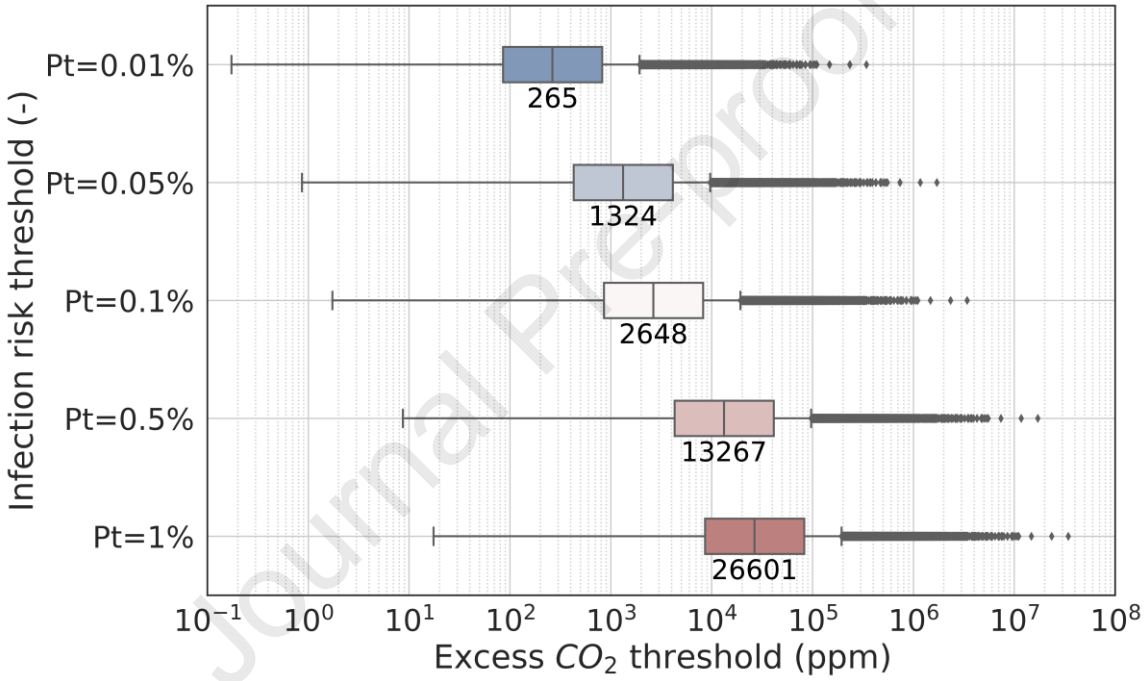

Figure 2. Excess CO_2 thresholds for the classroom (see Table 2) under different infection risk thresholds.

3.3 Effect of Initial Conditions

We have shown that initial condition of quanta and excess CO_2 can affect the derived safe excess CO_2 threshold when infection ratio varies among the occupancy stages. However, most previous studies overlook the initial condition of quanta and excess CO_2 in C_t derivation (Hou et al., 2021; Peng and Jimenez, 2021; Rudnick and Milton, 2003). To further quantify the

impact of initial condition of quanta/excess CO_2 on C_t when infection ratio varies, we compare two cases: 1) considering the initial condition of quanta/excess CO_2; 2) no initial quanta/excess CO_2. We consider two cases with the same indoor volume of 300 m^3, being occupied both with two stages. The occupants in the two cases are assumed to have "sedentary activity – breathing", and only 1 infector is adopted.

Case 1 assumes there are 20 occupants in Stage 1, and the occupant number in Stage 2 changes to 5, 10, 20, 40, 80 respectively, which means the infection ratio will change from 1/20 (Stage 1) to 1/5, 1/10, 1/20, 1/40, 1/80 (Stage 2) accordingly and initial quanta/excess CO_2 can affect C_t in Stage 2 in varying degrees. Case 2 assumes there are no occupants in Stage 1 (hence no initial quanta/excess CO_2), and 5 different occupancy levels are assumed for Stage 2 just like case 1. Here we aim to derive C_t for Stage 2 for both two cases with consideration of the impacts of initial quanta/excess CO_2 from Stage 1 (case 1) and without (case 2). The differences of results between the two cases can be used to quantify the impact of initial quanta/excess CO_2 on C_t. It's easy to derive C_t for case 2 as there are no initial quanta/excess CO_2, while for case 1, an estimation of initial quanta/excess CO_2 released from stage 1 is needed. Considering the excess CO_2 concentration is affected by different factors such as exposure time and ACH during Stage 1, here we assumed a constant value for initial excess CO_2 concentration for Stage 2 in case 1, namely, 1000 ppm. Initial quanta can then be derived based on it and infection ratios of Stage 1 (see Eq. S4 in Supplementary).

Figure 3 shows there are distinct differences of derived C_t between the cases with and without considering initial quanta/excess CO_2 when infection ratio of Stage 2 differs from Stage 1 (1/20), suggesting the initial condition of quanta/excess CO_2 shouldn't be ignored in

343 C_t derivation. Overall, when infection ratio increases (larger than 1/20) from Stage 1, C_t
344 considering initial condition is larger than that without considering initial quanta/excess CO_2,
345 and vice versa. The difference will be higher when the infection ratio deviates more from the
346 base case of 1/20. When the infection ratio increases from 1/20 (Stage 1) to 1/5 (Stage 2), C_{t50}
347 increases by 60 ppm than that without considering initial quanta/excess CO_2 and when the
348 Stage 2 infection ratio decreases from 1/20 to 1/80, C_{t50} becomes 260 ppm lower.

349

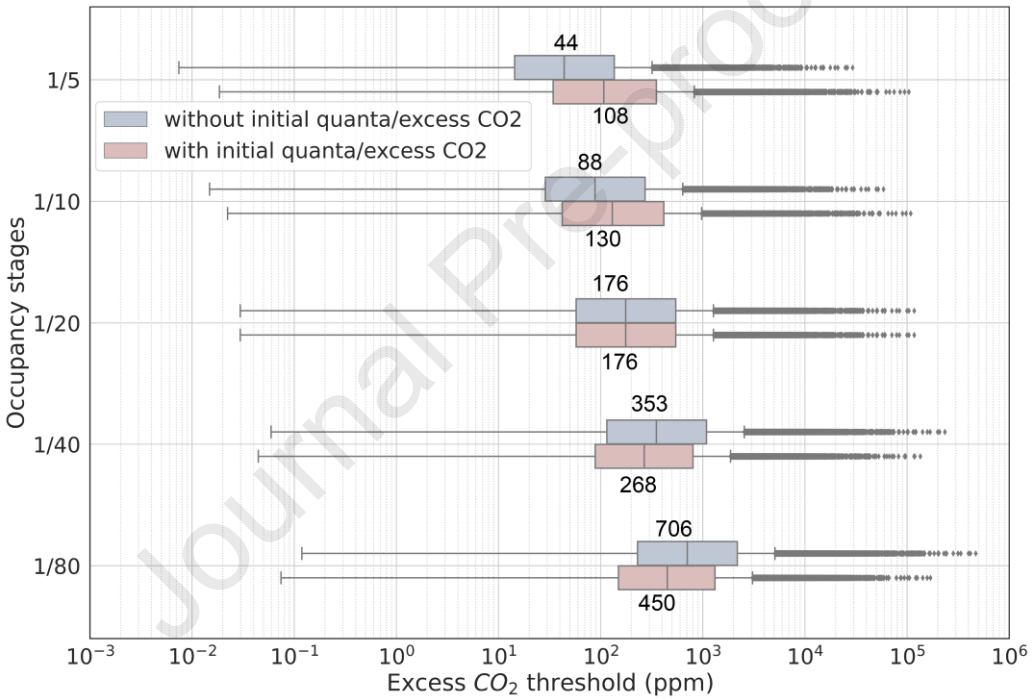

350 **Figure 3.** Excess CO_2 threshold of the second occupancy stage of an indoor space (300 m^3)
351 under different infection ratios considering with and without initial quanta/CO_2

352 **4. Discussion**

353 *4.1. New understanding of rebreathed-fraction model*

354 RF-based Wells-Riley model proposed by Rudnick and Milton's (2003) used CO_2 as a maker

for exhaled-breath exposure and avoided ACH estimation for airborne infection risk assessment. The model does not require any knowledge about ACH, hence it has been widely used in assessing airborne infection risk (Andrews et al., 2014; Hella et al., 2017; Richardson et al., 2014; Wood et al., 2014; Zürcher et al., 2020). However, However, we proved that RF-based model should be only adopted for spaces with fixed occupancy otherwise initial quanta will cause bias of it (see Part 3.3), but this is largely overlooked by many other studies. For spaces with varying occupancy, the initial quanta/excess CO_2 generated by previous occupants but remaining in the air can be very important determining the overall quanta/excess CO_2 concentration for next-stage occupancy. How will RF-based model deal with initial quanta/excess CO_2 for spaces with changing occupancy has not been adequately discussed before. In this article, we made analytical derivation to explain the mechanism of RF-based method in dealing with initial quanta/excess CO_2. We showed that initial quanta/excess CO_2 can be considered within the RF-based method in C_t derivation for Scenario 1 (with fixed occupancy) and Scenario 2 (with changing occupancy but fixed infection ratios). This further extends the generalization of RF-based model from spaces with fixed occupancy to spaces with changing occupancy. It should be noted that other recent studies (Burridge et al., 2021; Vouriot et al., 2021) resonate with our study in that they apply RF-based model to spaces with varying occupancy levels to assess infection risk. However, only two occupancy modes were considered in these studies, occupied and non-occupied, which are both included in our Scenario 1. In this contribution, we have proved that for spaces with both occupied and non-occupied modes, the non-occupied period does not affect the proportion of quanta concentration to excess CO_2 concentration in future occupied period if infection ratios remain

unchanged given only ventilation is considered here (see Supplementary Information).

4.2. Implications for C_t determination

Great uncertainty in C_t can be caused by the uncertainty of emissions (E_q and E_{CO2}) (see Figure 1). E_{CO2} and E_q contain uncertainty because they have interindividual variation and can be affected by factors such as age, gender (Buonanno et al., 2020a; Persily and de Jonge, 2017; Good et al., 2021). The value of E_q can vary by up to 3 orders of magnitude (e.g., 0.32-240 quanta/h for speaking under light activity) (Buonanno et al., 2020a) while E_{CO2} varies within only one order of magnitude (e.g., 2.88-43.2 L/h) (Persily and de Jonge, 2017). Different studies adopted very different values of E_q and therefore could lead to very different C_t. For only the classroom settings with the same activity level, the median value of E_q in our study is 0.37 quanta/h (Buonanno et al., 2020a), while it was in the range of 27.55 quanta/h to 100 quanta/h in other studies (Bazant et al., 2021; Hou et al., 2021; Peng and Jimenez, 2021), resulting in several hundred times lower C_t than our results.

The choice of P_t and I_i have also an impact C_t. Theoretically, lower P_t can promise safer indoor environment, but this would come at the cost of very low C_t practically impossible to achieve in real-world scenarios. E.g., a low level of C_t may require a very high ACH, unfeasible and prone to cause large energy cost due to the diminishing return phenomenon of ventilation (Li et al., 2021). Besides, how to determine the infector number I_i is also important as it is related to the total quanta emission. Our study defined I_i to be the maximum value of $\{1, P_I N_i\}$ as the worst-case scenario. On the contrary, Bazant et al. (2021) considered I_i to be the minimum value of $\{1, P_I N_i\}$, which resulted in a dramatically large C_t (even larger than 10000

ppm) when P_I is small.

4.3. Implications for infection risk monitoring and control

Our model has practical significance for indoor transmission monitoring and control. For Scenario 1 and Scenario 2, safe excess CO_2 threshold is related to variables such as occupancy level, duration and risk threshold through simple equations (see Equation (9) and Equation (12)), making it possible to apply our model for infection risk monitoring in Scenario 1 and 2 for public individuals. For instance, when arriving at a space such as a shopping center (as our Scenario 2), people can easily measure the indoor excess CO_2 level first through a portable low-cost CO_2 sensor, then by replacing C_t in Equation (12) by the measured data, people can roughly obtain a safe exposure duration for that shopping center based on their acceptable risk threshold to guide how long they should stay in the shopping center. Furthermore, taking into account the impact of initial quanta/excess CO_2 on risk estimation and C_t derivation, our model can be adopted to further develop different ventilation control strategies such as CO_2-based demand-controlled ventilation (Li and Cai, 2022) or intermittent ventilation strategy (Melikov et al., 2020; Zhang et al., 2022) with an objective to reduce indoor transmission risk by treating indoor excess CO_2 as a control variable.

Further applying our calculation framework into real-world scenarios, some insights can be gained by comparing derived C_t with measurement data/standard limits. For Scenario 1, the occupant numbers can largely affect C_t level, thus, it's warranted to concurrently consider CO_2 level and occupant level in transmission risk evaluation of an indoor environment. For example, for classrooms in Scenario 1, the measured excess CO_2 level was found to be in the range of

300 - 2500 ppm (outdoor level of 420 ppm) dependent on the number of occupants (Bakó-Biró et al., 2012; Vouriot et al., 2021; Persily et al., 2022). According to our framework, 300 ppm can represent an unsafe environment if the occupant number is less than 33, and 2500 ppm can still be a safe level if occupants is larger than 278. Therefore, C_t threshold should be used in conjunction with occupant number. For scenario 2, community prevalence can dominate C_t and can be used as a reference for lockdown policy implementation. It was found that the one-hour average CO_2 level of 40% shopping mall in Hong Kong exceeded 1000 ppm (Li et al., 2001). To keep infection risk no more than 0.01% for shopping malls, a community prevalence of less than 0.09% is needed according to our calculation framework, otherwise, such places should be locked down. For Scenario 3, taking a restaurant (~350 m^3) for example, considering two occupancy stage (N_1 = 20 for Stage 1 and N_2 = 80 for Stage 2) (Shen et al., 2021), according to ASHRAE 62.1 (ASHRAE, 2019), the maximum excess CO_2 limits (the steady-state excess CO_2 concentration under the required ventilation rate) for the first two occupancy stages are 540 ppm (Stage 1) and 790 ppm (Stage 2) respectively. But C_t calculated from our framework amounts to 180 ppm and 610 ppm, respectively. The difference indicates the target of infection risk control should be integrated into present ventilation standards to promise both a high level of IAQ and a low infection risk.

4.4. Limitation of the study

Our study is based on the assumption that outdoor ventilation is the only loss mechanism for quanta in Scenario 1 and Scenario 2, which results in a constant proportion between quanta concentration and excess CO_2 concentration, hence making RF-based model suitable for

deriving C_t for Scenario 1 and 2. However, surface deposition, filtration and virus deactivation could significantly contribute to reduce quanta concentration (Blocken et al., 2021; Su et al., 2021; van Doremalen et al., 2020). Neglecting these loss mechanisms may overestimate indoor quanta concentration and result in a lower estimate of C_t than needed. However, the reliability of the derived C_t for a safe indoor environment would not be affected.

The thresholds we derived are based on the assumption of a well-mixed room air. Thus, the location of CO_2 sensors needs to be carefully selected to adequately reflect indoor CO_2 conditions (Mahyuddin and Awbi, 2010; Mahyuddin et al., 2014). Additionally, our results only account for long-range airborne transmission neglecting the contribution of short-range transmission (Chen et al., 2021; Gao et al., 2021; Li, 2021). Limiting to monitoring infection risk based on C_t values may not be sufficient. Other intervention measures such as wearing masks and social distancing should be jointly considered to control indoor airborne transmission (Jarvis, 2020; Mittal et al., 2020a; Wagner et al., 2021).

Another limitation lies in the application of community prevalence (P_I) in our study. For scenario 1 and scenario 3, P_I is used to determine the indoor infector number, which would cause bias because 1) P_I might be smaller than the real value due to the asymptomatic characteristic of SARS-CoV-2 (Lee et al., 2020; Pollock and Lancaster, 2020); and 2) positive individuals may not be present at public spaces due to mandatory quarantine policy which would lead to a lower indoor infection ratio than P_I. For scenario 2, simply using P_I to represent the indoor infection ratio can lead to underestimate the real indoor infection ratio when the number of occupants is small. Conducting field measurement to estimate the average

461 occupancy level (N_{ave}) and selecting the maximum value of {1, $N_{ave}P_I$} could be an alternative
462 method for defining a convincible infection ratio for scenario 2. In addition, considering P_I is
463 changing during different time periods of pandemic, the indoor infection ratio would need to
464 be updated accordingly.

465 In addition, the uncertainty of C_t estimated by our study may be limited as we only
466 considered the uncertainty in emission settings (i.e., quanta emission rate, CO_2 emission rate)
467 in C_t derivation. Community prevalence P_I may contain uncertainty due to the reasons
468 mentioned above. The uncertainty of it may increase the uncertainty of C_t for Scenario 2 where
469 P_I is a dominating input in C_t derivation, but it may not obviously affect C_t for Scenario 1 and
470 3 because P_I is adopted in C_t derivation only when $P_I N_i > 1$ but the occupancy level (N_i) of
471 most cases in Scenario 1 and 3 is usually low and hence $P_I N_i < 1$. Similar as emission settings,
472 breathing rate can also contain uncertainty due to interindividual differences and factors such
473 as age and gender. In addition, quanta emission rate, CO_2 emission rate and breathing rate may
474 all be correlated to each other (Good et al., 2021). In our study, we simply adopted constant
475 breathing rates for different physical activity levels following the study of Buonanno et al.
476 (2020a) which estimated the quanta emission rate under different physical activity levels.
477 Quanta emission rate and CO_2 emission rate are also inter-related through physical activity
478 level (See Table 1). In future, based on more accurate data, the uncertainty and correlation of
479 those parameters may be further interpreted, and the uncertainty of C_t can be therefore further
480 estimated.

481 **5. Conclusion**

A new calculation framework was proposed in this study for deriving safe excess CO_2 threshold (C_t) for different spaces with consideration of initial quanta/excess CO_2 and fixed/changing occupancy levels. From our derivation process we found that the proportion of indoor excess CO_2 concentration to quanta concentration is constant for a constant infection ratio (infectors/occupants) of an indoor space. Based on this relationship, RF-based (rebreathed fraction-based) model can be directly applied for infection risk assessment and C_t derivation when infection ratio is constant, but not applicable for the cases with varying infection ratios.

Affected by factors such as occupant number (N_i), community prevalence (P_I) and activity level, the median value C_{t50} derived by our framework varies significantly among the selected cases, with a minimum value of 7 ppm for gym to a maximum value of 890 ppm for lecture hall, with long-tailed distributions. Initial quanta/excess CO_2 is found to largely affect C_t especially when the infection ratio varies significantly among the occupancy stages. A bias of several hundred ppm (e.g., 260 ppm for a space of 300 m^3 and with sedentary activity level) could be made if the initial quanta in C_t derivation is not well considered. Our finding illustrates that different CO_2 thresholds should be derived for different spaces and different occupancy stages, rather than being fixed at a constant value for all spaces.

Large uncertainty was also found in derived thresholds for all cases, spanning approximately 6 orders of magnitude, which are mainly influenced by quanta emission rate (E_q) and CO_2 emission rate (E_{CO2}). For a better control of indoor infection risk through CO_2 monitoring, more accurate input parameters would be needed.

Acknowledgement

XL acknowledged the financial support from China Scholarship Council (CSC) for pursuing her PhD at the University of Reading, UK.

References

Adams, W.C., 1993. Measurement of Breathing Rate and Volume in Routinely Performed Daily Activities. Final Report. Human Performance Laboratory, Physical Education Department, University of California, Davis. Human Performance Laboratory, Physical Education Department, University of California, Davis. Prepared for the California Air Resources Board, Contract No. A033-205, April 1993.

Ainsworth, B.E., Haskell, W.L., Whitt, M.C., Irwin, M.L., Swartz, A.M., Strath, S.J., O'Brien, W.L., Bassett, J., Schmitz, K.H., Emplaincourt, P.O., Jacobs, J., Leon, A.S., 2000. Compendium of physical activities: An update of activity codes and MET intensities. Med Sci Sports Exerc 32. https://doi.org/10.1097/00005768-200009001-00009

Andrews, J.R., Morrow, C., Walensky, R.P., Wood, R., 2014. Integrating social contact and environmental data in evaluating tuberculosis transmission in a South African township. Journal of Infectious Diseases 210, 597–603. https://doi.org/10.1093/infdis/jiu138

ASHRAE, 2019. ANSI/ASHRAE Standard 62.1-2019, Ventilation for acceptable indoor airquality. Peachtree Corners, GA: ASHRAE.

Bakó-Biró, Z., Clements-Croome, D.J., Kochhar, N., Awbi, H.B., Williams, M.J., 2012. Ventilation rates in schools and pupils' performance. Build Environ 48, 215–223. https://doi.org/10.1016/j.buildenv.2011.08.018

Bazant, M.Z., Kodio, O., Cohen, A.E., Khan, K., Gu, Z., Bush, J.W.M., 2021. Monitoring carbon dioxide to quantify the risk of indoor airborne transmission of COVID-19. Flow 1, 1–17. https://doi.org/10.1017/flo.2021.10

Blocken, B., van Druenen, T., Ricci, A., Kang, L., van Hooff, T., Qin, P., Xia, L., Ruiz, C.A., Arts, J.H., Diepens, J.F.L., Maas, G.A., Gillmeier, S.G., Vos, S.B., Brombacher, A.C., 2021. Ventilation and air cleaning to limit aerosol particle concentrations in a gym during the COVID-19 pandemic. Building and Environment 193, 107659. https://doi.org/10.1016/j.buildenv.2021.107659

Buonanno, G., Morawska, L., Stabile, L., 2020a. Quantitative assessment of the risk of airborne transmission of SARS-CoV-2 infection : Prospective and retrospective applications. Environ Int 145, 106112. https://doi.org/10.1016/j.envint.2020.106112

Buonanno, G., Stabile, L., Morawska, L., 2020b. Estimation of airborne viral emission : Quanta emission rate of SARS-CoV-2 for infection risk assessment. Environ Int 141, 105794. https://doi.org/10.1016/j.envint.2020.105794

Burridge, H.C., Fan, S., Jones, R.L., Noakes, C.J., Linden, P.F., 2021. Predictive and retrospective modelling of airborne infection risk using monitored carbon dioxide. Indoor and Built Environment 1420326X2110435. https://doi.org/10.1177/1420326x211043564

CDC, 2021. Ventilation in buildings. Atlanta: Centers for Disease Control and Prevention. https://www.cdc.gov/coronavirus/2019-ncov/community/ventilation.html

Chen, N., Zhou, M., Dong, X., Qu, J., Gong, F., Han, Y., Qiu, Y., Wang, J., Liu, Y., Wei, Y., Xia, J., Yu, T., Zhang, X., Zhang, L., 2020. Epidemiological and clinical characteristics of 99

cases of 2019 novel coronavirus pneumonia in Wuhan, China: a descriptive study. The Lancet 395, 507–513. https://doi.org/10.1016/S0140-6736(20)30211-7

Chen, W., Qian, H., Zhang, N., Liu, F., Liu, L., Li, Y., 2022. Extended short-range airborne transmission of respiratory infections. J Hazard Mater 422. https://doi.org/10.1016/j.jhazmat.2021.126837

CIBSE, C., 2020. COVID-19 Ventilation Guidance. https://www.cibse.org/Coronavirus-COVID-19

Dai, H., Zhao, B., 2020. Association of the infection probability of COVID-19 with ventilation rates in confined spaces. Build Simul 13, 1321–1327. https://doi.org/10.1007/s12273-020-0703-5

EMG/SPI-B, 2021. Application of CO2 monitoring as an approach to managing ventilation to mitigate SARS-CoV-2 transmission. https://www.gov.uk/government/publications/emg-and-spi-b-application-of-co2-monitoring-as-an-approach-to-managing-ventilation-to-mitigate-sars-cov-2-transmission-27-may-2021

Fang, K.-T., Li, R., Sudjianto, A., 2005. Design and Modeling for Computer Experiments (1st ed.). Chapman and Hall/CRC. https://doi.org/10.1201/9781420034899

Furuya, H., Nagamine, M., Watanabe, T., 2009. Use of a mathematical model to estimate tuberculosis transmission risk in an Internet café. Environ Health Prev Med 14, 96–102. https://doi.org/10.1007/s12199-008-0062-9

Gao, C.X., Li, Y., Wei, J., Cotton, S., Hamilton, M., Wang, L., Cowling, B.J., 2021. Multi-route respiratory infection: When a transmission route may dominate. Science of the Total Environment 752, 141856. https://doi.org/10.1016/j.scitotenv.2020.141856

Gammaitoni, L., Nucci, M. C., 1997. Using a mathematical model to evaluate the efficacy of TB control measures. Emerging infectious diseases, 3(3), 335–342. https://doi.org/10.3201/eid0303.970310

Good, N., Fedak, K.M., Goble, D., Keisling, A., L'Orange, C., Morton, E., Phillips, R., Tanner, K., Volckens, J., 2021. Respiratory Aerosol Emissions from Vocalization: Age and Sex Differences Are Explained by Volume and Exhaled CO2. Environ Sci Technol Lett 8, 1071–1076. https://doi.org/10.1021/acs.estlett.1c00760

Hella, J., Morrow, C., Mhimbira, F., Ginsberg, S., Chitnis, N., Gagneux, S., Mutayoba, B., Wood, R., Fenner, L., 2017. Tuberculosis transmission in public locations in Tanzania: A novel approach to studying airborne disease transmission. Journal of Infection 75, 191–197. https://doi.org/10.1016/j.jinf.2017.06.009

Hou, D., Katal, A., Wang, L. (Leon), Katal1, A., Wang, L. (Leon), 2021. Bayesian Calibration of Using CO2 Sensors to Assess Ventilation Conditions and Associated COVID-19 Airborne Aerosol Transmission Risk in Schools. medRxiv 2021.01.29.21250791.

Jarvis, M.C., 2020. Aerosol Transmission of SARS-CoV-2: Physical Principles and Implications. Front Public Health. https://doi.org/10.3389/fpubh.2020.590041

Jia, W., Wei, J., Cheng, P., Wang, Q., Li, Y., 2022. Exposure and respiratory infection risk via the short-range airborne route. Build Environ 219. https://doi.org/10.1016/j.buildenv.2022.109166

Jones, B., Sharpe, P., Iddon, C., Hathway, E.A., Noakes, C.J., Fitzgerald, S., 2021. Modelling uncertainty in the relative risk of exposure to the SARS-CoV-2 virus by airborne aerosol transmission in well mixed indoor air. Build Environ 191.

https://doi.org/10.1016/j.buildenv.2021.107617

Ke, R., Zitzmann, C., Ho, D. D., Ribeiro, R. M., and Perelson, A. S.: In vivo kinetics of SARS-CoV-2 infection and its relationship with a person's infectiousness, Proc. Natl. Acad. Sci. U. S. A., 118, https://doi.org/10.1073/pnas.2111477118, 2021.

Ke, R., Martinez, P. P., Smith, R. L., Gibson, L. L., Mirza, A., Conte, M., Gallagher, N., Luo, C. H., Jarrett, J., Zhou, R., Conte, A., Liu, T., Farjo, M., Walden, K. K. O., Rendon, G., Fields, C. J., Wang, L., Fredrickson, R., Edmonson, D. C., Baughman, M. E., Chiu, K. K., Choi, H., Scardina, K. R., Bradley, S., Gloss, S. L., Reinhart, C., Yedetore, J., Quicksall, J., Owens, A. N., Broach, J., Barton, B., Lazar, P., Heetderks, W. J., Robinson, M. L., Mostafa, H. H., Manabe, Y. C., Pekosz, A., McManus, D. D., and Brooke, C. B.: Daily longitudinal sampling of SARS-CoV-2 infection reveals substantial heterogeneity in infectiousness, Nat Microbiol, 7, 640-652, 2022.

Li, B., Cai, W., 2022. A novel CO2-based demand-controlled ventilation strategy to limit the spread of COVID-19 in the indoor environment. Build Environ 219. https://doi.org/10.1016/j.buildenv.2022.109232

Lee, S., Kim, T., Lee, E., Lee, C., Kim, H., Rhee, H., Park, S.Y., Son, H.J., Yu, S., Park, J.W., Choo, E.J., Park, S., Loeb, M., Kim, T.H., 2020. Clinical Course and Molecular Viral Shedding among Asymptomatic and Symptomatic Patients with SARS-CoV-2 Infection in a Community Treatment Center in the Republic of Korea. JAMA Intern Med 180, 1447–1452. https://doi.org/10.1001/jamainternmed.2020.3862

Lelieveld, J., Helleis, F., Borrmann, S., Cheng, Y., Drewnick, F., Haug, G., Klimach, T., Sciare, J., Su, H., Pöschl, U., 2020. Model calculations of aerosol transmission and infection risk of covid-19 in indoor environments. Int J Environ Res Public Health 17, 1–18. https://doi.org/10.3390/ijerph17218114

Li, W.M., Lee, S.C., Chan, L.Y., 2001. Indoor air quality at nine shopping malls in Hong Kong. Science of The Total Environment 273, 27–40. https://doi.org/10.1016/S0048-9697(00)00833-0

Li, Y., 2021. Basic routes of transmission of respiratory pathogens—A new proposal for transmission categorization based on respiratory spray, inhalation, and touch. Indoor Air. https://doi.org/10.1111/ina.12786

Li, Y., Cheng, P., Jia, W., 2021. Poor ventilation worsens short-range airborne transmission of respiratory infection. Indoor Air. https://doi.org/10.1111/ina.12946

Ma, Y., Horsburgh, C.R., White, L.F., Jenkins, H.E., 2018. Quantifying TB transmission: A systematic review of reproduction number and serial interval estimates for tuberculosis. Epidemiol Infect 146, 1478–1494. https://doi.org/10.1017/S0950268818001760

Mahyuddin, N., Awbi, H., 2010. The spatial distribution of carbon dioxide in an environmental test chamber. Build Environ 45, 1993–2001. https://doi.org/10.1016/j.buildenv.2010.02.001

Mahyuddin, N., Awbi, H.B., Alshitawi, M., 2014. The spatial distribution of carbon dioxide in rooms with particular application to classrooms. Indoor and Built Environment 23, 433–448. https://doi.org/10.1177/1420326X13512142

Melikov, A.K., Ai, Z.T., Markov, D.G., 2020. Intermittent occupancy combined with ventilation: An efficient strategy for the reduction of airborne transmission indoors.

631 Science of the Total Environment 744. https://doi.org/10.1016/j.scitotenv.2020.140908
632 Mihi, Mirela, Ani, I.-D., Mihi, M, Professor, F., Ani, I., Kursan Milaković, I., Professor, A.,
633 2018. Time spent shopping and consumer clothing purchasing behaviour EKONOMSKI
634 PREGLED.
635 Miller, S.L., Nazaroff, W.W., Jimenez, J.L., Boerstra, A., Buonanno, G., Dancer, S.J., Kurnitski,
636 J., Marr, L.C., Morawska, L., Noakes, C., 2021. Transmission of SARS-CoV-2 by
637 inhalation of respiratory aerosol in the Skagit Valley Chorale superspreading event. Indoor
638 Air 31, 314–323. https://doi.org/10.1111/ina.12751
639 Mittal, R., Meneveau, C., Wu, W., 2020a. A mathematical framework for estimating risk of
640 airborne transmission of COVID-19 with application to face mask use and social
641 distancing. Physics of Fluids 32. https://doi.org/10.1063/5.0025476
642 Mittal, R., Ni, R., Seo, J.H., 2020b. The flow physics of COVID-19. J Fluid Mech 894.
643 https://doi.org/10.1017/jfm.2020.330
644 Molina, C., Jones, B., 2021. Investigating Uncertainty in the Relationship between Indoor
645 Steady-State CO2 Concentrations and Ventilation Rates. Aivc.
646 https://doi.org/10.13140/RG.2.2.16867.99361
647 Peng, Z., Jimenez, J.L., 2021. Exhaled CO2as a COVID-19 infection risk proxy for different
648 indoor environments and activities. Environ Sci Technol Lett 8, 392–397.
649 https://doi.org/10.1021/acs.estlett.1c00183
650 Peng, Z., Rojas, A. L. P., Kropff, E., Bahnfleth, W., Buonanno, G., Dancer, S. J., Kurnitski, J.,
651 Li, Y., Loomans, M. G. L. C., Marr, L. C., Morawska, L., Nazaroff, W., Noakes, C., Querol,
652 X., Sekhar, C., Tellier, R., Greenhalgh, T., Bourouiba, L., Boerstra, A., Tang, J. W., Miller,
653 S. L., and Jimenez, J. L.: Practical Indicators for Risk of Airborne Transmission in Shared
654 Indoor Environments and Their Application to COVID-19 Outbreaks, Environ. Sci.
655 Technol., 56, 1125-1137, 2022.
656 Persily, A., de Jonge, L., 2017. Carbon dioxide generation rates for building occupants. Indoor
657 Air 27, 868–879. https://doi.org/10.1111/ina.12383
658 Persily, A., Bahnfleth, W., Kipen, H., Lau, J., Mandin, C., Sekhar, C., Wagocki, P. and Nguyen
659 Weekes, L.,2022, ASHRAE's New Position Document on Indoor Carbon
660 Dioxide,ASHRAE,Journal,
661 https://tsapps.nist.gov/publication/get_pdf.cfm?pub_id=934476
662 Riley, E. C., Murphy, G., Riley, R. L., 1978. Airborne spread of measles in a suburban
663 elementary school. American journal of epidemiology, 107(5), 421–432.
664 https://doi.org/10.1093/oxfordjournals.aje.a112560
665 Pollock, A.M., Lancaster, J., 2020. Asymptomatic transmission of covid-19. The BMJ.
666 https://doi.org/10.1136/bmj.m4851
667 Pouwels, K.B., et al., 2021. Community prevalence of SARS-CoV-2 in England from April to
668 November, 2020: results from the ONS Coronavirus Infection Survey. The Lancet Public
669 Health 6, e30–e38. https://doi.org/10.1016/S2468-2667(20)30282-6
670 Qian, H., Miao, T., Liu, L., Zheng, X., Luo, D., Li, Y., 2021. Indoor transmission of SARS-
671 CoV-2. Indoor Air 31, 639–645. https://doi.org/10.1111/ina.12766
672 Rudnick, S.N., Milton, D.K., 2003. Risk of indoor airborne infection transmission estimated
673 from carbon dioxide concentration. Indoor Air 13, 237–245.
674 https://doi.org/10.1034/j.1600-0668.2003.00189.x

675 REHVA, 2021. REHVA COVID-19 Guidance, version 4.1. Brussels, Belgium: Federation of
676 European Heating, Ventilation and Air Conditioning Associations.
677 https://www.rehva.eu/fileadmin/user_upload/REHVA_COVID-
678 19_guidance_document_V4.1_15042021.pdf
679 Richardson, E.T., Morrow, C.D., Kalil, D.B., Bekker, L.G., Wood, R., 2014. Shared air: A
680 renewed focus on ventilation for the prevention of tuberculosis transmission. PLoS One
681 9, 1–7. https://doi.org/10.1371/journal.pone.0096334
682 SAGE-EMG, 2020. EMG: Role of ventilation in controlling SARS-CoV-2 transmission.
683 https://www.gov.uk/government/publications/emg-role-of-ventilation-in-controllingsars-
684 cov-2-transmission-30-september-2020
685 Shen, J., Kong, M., Dong, B., Birnkrant, M.J., Zhang, J., 2021. A systematic approach to
686 estimating the effectiveness of multi-scale IAQ strategies for reducing the risk of airborne
687 infection of SARS-CoV-2. Build Environ 200.
688 https://doi.org/10.1016/j.buildenv.2021.107926
689 Sobol', I.M., 1994. A Primer for the Monte Carlo Method (1st ed.). CRC Press.
690 https://doi.org/10.1201/9781315136448
691 Su, A., Grist, S.M., Geldert, A., Gopal, A., Herr, A.E., 2021. Quantitative UV-C dose validation
692 with photochromic indicators for informed N95 emergency decontamination. PLoS ONE
693 16, 1–24. https://doi.org/10.1371/journal.pone.0243554
694 van Doremalen, N., Bushmaker, T., Morris, D.H., Holbrook, M.G., Gamble, A., Williamson,
695 B.N., Tamin, A., Harcourt, J.L., Thornburg, N.J., Gerber, S.I., Lloyd-Smith, J.O., de Wit,
696 E., Munster, V.J., 2020. Aerosol and Surface Stability of SARS-CoV-2 as Compared with
697 SARS-CoV-1. New England Journal of Medicine 382, 1564–1567.
698 https://doi.org/10.1056/nejmc2004973
699 Vouriot, C.V.M., Burridge, H.C., Noakes, C.J., Linden, P.F., 2021. Seasonal variation in
700 airborne infection risk in schools due to changes in ventilation inferred from monitored
701 carbon dioxide. Indoor Air 31, 1154–1163. https://doi.org/10.1111/ina.12818
702 Wagner, J., Sparks, T.L., Miller, S., Chen, W., Macher, J.M., Waldman, J.M., 2021. Modeling
703 the impacts of physical distancing and other exposure determinants on aerosol
704 transmission. J Occup Environ Hyg 1–15.
705 https://doi.org/10.1080/15459624.2021.1963445
706 Wei, J., Li, Y., 2016. Airborne spread of infectious agents in the indoor environment. Am J
707 Infect Control 44, S102–S108. https://doi.org/10.1016/j.ajic.2016.06.003
708 Wood, R., Morrow, C., Ginsberg, S., Piccoli, E., Kalil, D., Sassi, A., Walensky, R.P., Andrews,
709 J.R., 2014. Quantification of shared air: A Social and environmental determinant of
710 airborne disease transmission. PLoS One 9, 1–8.
711 https://doi.org/10.1371/journal.pone.0106622
712 Zhang, S., Ai, Z., Lin, Z., 2021. Occupancy-aided ventilation for both airborne infection risk
713 control and work productivity. Build Environ 188.
714 https://doi.org/10.1016/j.buildenv.2020.107506
715 Zhang, S., Niu, D., Lin, Z., 2022. Occupancy-aided ventilation for airborne infection risk
716 control: Continuously or intermittently reduced occupancies? Build Simul.
717 https://doi.org/10.1007/s12273-022-0951-7
718 Zürcher, K., Morrow, C., Riou, J., Ballif, M., Koch, A.S., Bertschinger, S., Liu, X., Sharma,

M., Middelkoop, K., Warner, D., Wood, R., Egger, M., Fenner, L., 2020. Novel approach to estimate tuberculosis transmission in primary care clinics in sub-Saharan Africa: Protocol of a prospective study. BMJ Open 10. https://doi.org/10.1136/bmjopen-2019-036214

Supplementary Information

Derivation Process for Scenario 1 and Scenario 2

Scenario 1 and Scenario 2 have constant infection ratios among different occupancy stages, specifically, $I_1/N_1 = I_2/N_2 = \ldots = I_i/N_i$.

For S_1 (the start occupancy stage) with no initial quanta and initial excess CO_2, the solved quanta concentration ($C_{q,1}$) and excess CO_2 concentration ($C_{CO2,1}$) over time T_1 through mass balance equations can be expressed as:

$$C_{q,1}(t) = -\frac{I_1 E_q}{\lambda_1 V} e^{-\lambda_1 t} + \frac{I_1 E_q}{\lambda_1 V} \tag{S1}$$

$$C_{CO2,1}(t) = -\frac{N_1 E_{CO2}}{\lambda_1 V} e^{-\lambda_1 t} + \frac{N_1 E_{CO2}}{\lambda_1 V} \tag{S2}$$

A fixed proportion between quanta and excess CO_2 during stage S_1 can be derived:

$$\frac{C_{q,1}(t)}{C_{CO2,1}(t)} = \frac{I_1}{N_1}\frac{E_q}{E_{\mathrm{CO2}}} \tag{S3}$$

Because initial quanta concentration ($C_{qin,2}$) and initial excess CO_2 concentration ($C_{cin,2}$) for next occupancy stage S_2 are exactly the concentrations at the end of S_1, thus, they also have the fixed proportion relationship as:

$$\frac{C_{qin,2}(t)}{C_{cin,2}(t)} = \frac{I_1}{N_1}\frac{E_q}{E_{\mathrm{CO2}}} \tag{S4}$$

For S_2 (second occupancy stage), replacing initial quanta concentration ($C_{qin,2}$) by initial excess CO_2 concentration ($C_{\mathrm{Cin},2}$) on basis of the fixed proportion above and a constant infection ratio of $I_1/N_1 = I_2/N_2$, quanta concentration and excess CO_2 concentration over time (T_2) can be expressed as:

$$C_{q,2}(t) = \frac{I_2}{N_2}\frac{E_q}{E_{\mathrm{CO2}}}((C_{\mathrm{Cin},2} - \frac{N_2 E_{CO2}}{\lambda_2 V})e^{-\lambda_2 t} + \frac{N_2 E_{CO2}}{\lambda_2 V}) \tag{S5}$$

$$C_{CO2,2}(t) = ((C_{\mathrm{Cin},2} - \frac{N_2 E_{CO2}}{\lambda_2 V})e^{-\lambda_2 t} + \frac{N_2 E_{CO2}}{\lambda_2 V} \tag{S6}$$

A same proportion between quanta and excess CO_2 concentration can be found during occupancy stage S_2:

$$\frac{C_{q,2}(t)}{C_{CO2,2}(t)} = \frac{I_2}{N_2}\frac{E_q}{E_{\mathrm{CO2}}} \tag{S7}$$

If there exists a stage S_0 following stage S_2 that without occupancy (no occupants indoor during period T_0), quanta and excess CO_2 remained by stage S_2 also experience a synchronously damping in fixed proportion as S_2:

$$C_{q,0}(t) = \frac{I_2}{N_2}\frac{E_q}{E_{\mathrm{co2}}}(C_{\mathrm{Cin},0}e^{-\lambda_0 t}) \tag{S8}$$

$$C_{CO2,0}(t) = C_{\mathrm{Cin},0}e^{-\lambda_0 t} \tag{S9}$$

$$\frac{C_{q,0}(t)}{C_{CO2,0}(t)} = \frac{I_2}{N_2}\frac{E_q}{E_{\mathrm{CO2}}} \tag{S10}$$

Based on constant infection ratios ($I_1/N_1 = I_2/N_2 = \ldots = I_i/N_i$), a general analytical expression for quanta

concentration and excess CO_2 concentration for stage S_i can be concluded from the derivation process above:

$$C_{q,i}(t) = \frac{I_i}{N_i}\frac{E_q}{E_{\mathrm{CO2}}}((C_{\mathrm{Cin,i}} - \frac{N_i E_{CO2}}{\lambda_i V})e^{-\lambda_i t} + \frac{N_i E_{CO2}}{\lambda_i V}) \quad \text{(S11)}$$

$$C_{CO2,i}(t) = (C_{\mathrm{Cin,i}} - \frac{N_i E_{CO2}}{\lambda_i V})e^{-\lambda_i t} + \frac{N_i E_{CO2}}{\lambda_i V} \quad \text{(S12)}$$

For all occupancy stages in Scenario 1 and Scenario 2, quanta concentration and excess CO_2 concentration possess a fixed proportion dominated by three parameters: (1) constant infection ratio; (2) constant quanta emission rate; (2) constant CO_2 emission rate.

$$\frac{C_{q,i}(t)}{C_{CO2,i}(t)} = \frac{I_i}{N_i}\frac{E_q}{E_{\mathrm{CO2}}} \quad \text{(S13)}$$

Replacing quanta concentration by excess CO_2 concentration, airborne infection risk for stage i can be quantified through Wells-Riley equation based on the excess CO_2 concentration:

$$P = 1 - e^{-B\frac{I_i}{N_i}\frac{E_q}{E_{\mathrm{CO2}}}\int_0^{T_i} C_{CO2,i}(t)dt} \quad \text{(S14)}$$

Equation (S14) can be converted directly into the classical rebreathed fraction-based infection risk model (Rudnick and Milton, 2003) with $BC_{co2}(t)/E_{\mathrm{co2}}$ representing the rebreathed fraction. Safe excess CO_2 threshold for occupancy stage S_i for Scenario 1 and Scenario 2 ($I_i/N_i = P_I$) can then be derived on basis of Equation (S14) with a predefined risk threshold P_t:

$$C_t = \frac{E_{CO2}N_i}{E_q T_i B I_i} ln\left(\frac{1}{1-P_t}\right) \quad \text{(S15)}$$

For each occupancy stage, the initial quanta released by previous stages has been considered in the derivation of safe excess CO_2 threshold in Equation (S15). The application of the derived CO_2 threshold can be extended to more general occupancy stages without limitation of no initial quanta in space.

Reference

Rudnick, S.N., Milton, D.K., 2003. Risk of indoor airborne infection transmission estimated from carbon dioxide concentration. Indoor Air 13, 237–245. https://doi.org/10.1034/j.1600-0668.2003.00189.x

Highlights

- Rebreathed fraction-based model can be applied for spaces with changing occupants but constant infection ratios.
- Initial quanta and excess CO_2 lead to bias of determining excess CO_2 threshold when infection ratio changes.
- Excess CO_2 threshold contains large uncertainty and should be determined on a case-by-case basis.

Declaration of interests

☐ The authors declare that they have no known competing financial interests or personal relationships that could have appeared to influence the work reported in this paper.

☒ The authors declare the following financial interests/personal relationships which may be considered as potential competing interests:

Xiaowei Lyu reports financial support was provided by China Scholarship Council.